Post-Print of Conference paper submitted to the
10th International Conference on Structural Health Monitoring of Intelligent Infrastructure,
30 June - 2 July, Porto, Portugal

Damage-sensitive features for rapid damage assessment in a seismic context

Yves Reuland[1], Panagiotis Martakis[1], Eleni Chatzi[1]
[1] Dept. of Civil, Environmental and Geomatic Engineering, ETH Zurich, Stefano-Franscini-Platz 5, CH-8093 Zurich
Email: reuland@ibk.baug.ethz.ch, martakis@ ibk.baug.ethz.ch, chatzi@ ibk.baug.ethz.ch

ABSTRACT: Rapid assessment is crucial for a prompt functional recovery of the built environment in the aftermath of disastrous earthquakes. Recent building codes have efficiently lowered the death toll of earthquakes, yet cracks and other kinds of accumulated damage are tolerated and can result in successively weakened structures, which eventually fail. In order to enhance the recovery capacity of communities, rapid damage assessment of the built infrastructure after a seismic event is necessary. Current post-earthquake practices rely on slow and potentially subjective visual inspections. Permanent monitoring installations are met mainly in exceptional cases of seismic prone regions, applied in structures of high importance, such as high-rise buildings. In recent years, however, a large variety of sensing solutions has become available at affordable cost, allowing the engineering community to envision permanent-monitoring applications even in conventional buildings. To this end, instrumented representative buildings can serve as indicators for properly defined building classes. When combined with adequate structural-health-monitoring techniques, sensor data recorded during earthquakes have the potential to provide an automated near-real-time detection of possible earthquake damage. However, damage detection in existing buildings is impaired by the presence of multiple non-structural components, a high redundancy in load-bearing elements, elastic non-linearities and the impact of potential localized failure mechanisms. Using a simulated case study of a masonry building, along with data from shake-table tests, the applicability of automated damage detection, through data-driven damage-sensitive features, is assessed, along with the potential for quantifying damage in order to proceed with smart-tagging of earthquake-damaged buildings.

KEY WORDS: Damage-Sensitive Features; Data-Driven Damage Assessment; Smart Tagging; Post-Earthquake Assessment.

1 INTRODUCTION

Despite improvements in building design codes and construction techniques, earthquakes still carry large potential to damage structures and to interrupt the functionality of the built environment. In addition, designing and retrofitting all buildings to withstand rare earthquakes having long return periods without sustaining any damage is non-viable for economical, ecological and technical reasons. Therefore, earthquakes will always result in a high demand for post-earthquake damage assessment.

Current approaches to post-earthquake assessment of buildings rely on expert-conducted visual inspections that, in addition to suffering from subjectivity, delay rapid recovery due to the time required to inspect large building stocks. However, recent advances in sensor development have resulted in increased availability of low cost sensors, thus making permanent monitoring installations a realistic outlook even for conventional buildings that consist the majority of the existing building stock. In this framework, use of modal properties derived from ambient vibrations have gained popularity to detect structural damage [1, 2]. However, ambient vibrations correspond to very low amplitudes of shaking and, thus, may not capture the nonlinear behavior of structures under large-amplitude shaking. Permanently installed sensors record the response of buildings to earthquake actions and provide valuable information regarding the state of a structure after the event.

Damage-sensitive features (DSF) are data-driven indicators of nonlinear behavior that can be derived from measured vibrations in near-real time and therefore constitute a valuable tool towards automated tagging of buildings after strong ground motions as either safe or unsafe. Well-designed DSFs detect the onset of damage and further provide information regarding its severity, which assists in the planning of recovery trajectories after catastrophic events, hence increasing the resilience of the built environment.

Many damage detection approaches based on modal properties, such as natural frequencies and mode shapes, have been applied and tested on high-rise buildings or bridges [3-5]. Such slender structures enable the modal identification of higher modes, which are often found to be most sensitive to damage. However, this does not fit the profile of low-rise masonry buildings, which present the most vulnerable elements in the European building stock. Such masonry buildings are often characterized by high lateral stiffness, local failure modes and redundancy in the lateral load-resisting system. Masonry buildings often exhibit a single dominant mode in each direction, and thus constitute a challenge for many existing approaches of damage detection. In addition, unlike steel or modern reinforced concrete structures that can be characterized as ductile, masonry buildings exhibit sudden and permanent stiffness changes, which results in a rather brittle behavior and requires DSFs that can pick up smallest changes in the modal behavior in short time windows.

In this contribution, four DSFs, tracking changes in the frequency-domain of the dominant mode, are compared using a simulated case study and shake-table tests. We demonstrate the potential of DSFs, which are computed in near-real time on the basis of measurable dynamic data, to reliably detect damage. In addition, an attempt is made to quantify damage through the correlation of DSFs with damage grades (DG) that are used in macro-seismic applications for quantifying damage of individual buildings within an entire region. It is shown that DSFs based on transmissibility and wavelet decomposition carry the potential to assist emergency responders with a rapid post-earthquake damage assessment.

2 DAMAGE-SENSITIVE FEATURES

In data-driven damage identification, damage-sensitive features (DSF) are derived from measured time series to assess the presence, extent and location of damage or nonlinearity. In this contribution, four DSFs, mutually exploiting the influence of stiffness-reduction (without changes to the mass distribution) on the fundamental frequency, are presented and their applicability is compared based on case studies. The frequency response of the structure is analyzed with three approaches, namely transmissibility, magnitude-square coherence and wavelet transforms.
Ideal DSFs are indicators of nonlinearity and thus, scale with the amount of nonlinearity that is sustained by a structure. On the other hand, DSFs should have little correlation with either the amplitude or the spectral content of the ground shaking. In this paper, the DSFs are assessed over the entire duration of an earthquake, thereby providing an average assessment of the dynamic response of the structure to an earthquake. Some of the presented DSFs can also be modified to be applied to data-windows, in order to track changes over time. However, this is outside the scope of this paper.

For the subsequent analysis, the input excitations is considered acting at the base while the measured output comprises exclusively recordings at the roof-top level of the structure. When positioning several sensors along the height of the building, DSFs can also be inferred locally and thus, enable to get insights into the location of the damage and into the severity of damage of subparts of the building. However, this falls outside the scope of this paper.

Based on the availability of affordable sensors that allow to measure large-amplitude vibrations, accelerations are considered as the most likely measurement data. Finally, results are reported for the fundamental frequency in the dominant direction of shaking, as higher modes may not always be available for low-rise and stiff structures, such as masonry buildings. However, the structure of the presented DSFs allows computing the same quantities for higher modes or any frequency range of interest.

2.1 Transmissibility-based features

Transmissibility is the unitless ratio between the power spectrum of the acceleration time series corresponding to an input signal and the power spectrum of the output signal, as noted in Eq. 1:

$$T_{i,o} = \frac{P_{oo}}{P_{ii}} \tag{1}$$

In Eq. 1, $T_{i,o}$ denotes the transmissibility between the input acceleration time series, $\ddot{x}_i$, and the output acceleration time series, $\ddot{x}_o$. P_{oo} is the power spectrum of the output signal andP_{ii} the power spectrum of the input signal. Peaks in the transmissibility function correspond to natural frequencies of a linear system and can therefore be used to track possible changes in the frequency domain due to damage.
In order to reveal changes in the fundamental frequency, which originate from changes in the stiffness of the system, transmissibility evaluations can be compared with a reference state considered undamaged. Comparison to the reference transmissibility, denotedT_{ref}, is performed using a measure of vector collinearity [6], known as modal assurance criterion (MAC) [7]. Thus, the transmissibility-based DSF, DSF_{tra}, is a scalar, derived using Eq. 2:

$$DSF_{tra} = \frac{\left|T_{ref}{}^{T} T_{eqk}\right|^2}{\left|T_{ref}{}^{t} T_{ref}\right| \left|T_{eqk}{}^{t} T_{eqk}\right|} \tag{2}$$

Where T_{ref} and T_{eqk} are the transmissibility vectors, corresponding to a given range of frequencies, for the reference and the earthquake signal respectively. $\cdot^T$ denotes the transpose of the transmissibility vector.

2.2 Features based on magnitude-squared coherence

The magnitude-squared coherence is traditionally used to track linear dependencies in the spectral decomposition of two signals [8]. In a similar way to the transmissibility, the magnitude-squared coherence is a unitless ratio which yields a value of 1 for linearly correlated signals. For an input time series, $\ddot{x}_i$, and output time series, $\ddot{x}_o$, the magnitude-squared coherence is calculated using Eq. 3:

$$C_{io} = \frac{|P_{io}|^2}{P_{ii}\, P_{oo}} \tag{3}$$

Based on a linear reference signal, which has a coherence close to 1, the change in coherence is again obtained as the MAC, as shown in Eq. 4:

$$DSF_{coh} = \frac{\left|C_{ref}{}^{t} C_{eqk}\right|^2}{\left|C_{ref}{}^{t} C_{ref}\right| \left|C_{eqk}{}^{t} C_{eqk}\right|} \tag{4}$$

2.3 Wavelet-based features

Wavelet decomposition is a powerful tool to represent changes in the frequency content of a signal over time. The wavelet transform decomposes a time-history into a sum of wavelets that are obtained by dilating, scaling and time-shifting a mother wavelet, in this case the Morlet wavelet. Two DSFs based on the wavelet decomposition of the structural response are assessed [9, 10]: DSF_{wte} based on the energy spread of the response signal in the frequency domain and DSF_{wtc} based on the centroid of the energy spread in the time domain (after the main shaking of the structure, corresponding to 95% of the cumulated energy of the earthquake).

Based on the fact that for buildings damage often corresponds to reduced stiffness, DSF_{wte} has been defined by Noh et al [9] as the ratio of the total energy at the fundamental frequency, E_{f1}, and the total energy E_{tot} at some discrete frequencies in the range between [f_1/2, f_1], as defined in Eq. 5:

$$DSF_{wte} = \frac{E_{f_1}}{E_{tot}} \tag{5}$$

As damage leads to a reduction of the natural frequencies, Noh et al. [9] defined another DSF, which measures the time of decay of energy in the response signal. Based on the assumption that lower natural frequencies lead to a longer decay in energy, this DSF_{wtc} is defined in Eq. 6:

$$DSF_{wtc} = \frac{\sum_{b=t_{95}/t_s}^{K} E_{f_1}(b) \cdot b \cdot t_s}{\sum_{b=t_{95}}^{K} E_{f_1}(b)} - t_{95} \quad (6)$$

Where t_{95} is the time to reach 95% of the total cumulated energy of the input shaking, $\ddot{x}_i$; $E_{f_1}(b)$ is the energy of the output $\ddot{x}_o$ at frequency f_1 at time sample b; t_s is the sampling period and K is the total number of samples that are measured.

2.4 Computing the damage-sensitive features

Various approaches exist to derive the power spectrum in the frequency domain of a time history. In this paper, Fourier analysis is used for very short and zero-padded time-windows in order to obtain the resolution in the frequency domain that is required for DSF_{tra} and DSF_{coh}, while still being able to detect small changes over time. In order to avoid numerical singularities in the Fourier analysis, short time windows containing highly transient signals are not considered in the analysis. Similarly, due to the ratios that define Equations 1 and 3, time windows for which the power spectrum of the input signal, P_{ii}, contains marked minima in the frequency range of interest (less than 5% of the average power spectrum of interest) are also discarded.

For the wavelet decomposition, the trade-off between precision in either the frequency or the time domain is chosen to reach higher precision in the frequency domain for DSF_{wte} and higher precision in the time domain for DSF_{wtc}, given the nature of the two wavelet-based DSFs.

3 DAMAGE-SENSITIVE FEATURES APPLIED TO SIMULATED BUILDING RESPONSES

In the following, the potential of DSFs to detect and quantify nonlinear behavior is studied through a simulated case study, based on a typical Swiss four-story masonry building that has been built in the early 20th century [11].

The building is modelled as a three-dimensional equivalent frame model in the Tremuri software [12, 13], where a dynamic nonlinear time-history analysis is carried out. The building slabs are considered to be rigid compared to the lateral stiffness of the walls and the building is assumed fixed at the ground level. As the goal of the simulations is not to reproduce an observed behavior, characteristic parameter values are used for material properties.

A nonlinear static (pushover) analysis is performed prior to the time-history analysis in order to establish the lateral load-resistance. The relation between roof displacement and base shear is provided in Figure 1. The bi-linear idealization of the curve results in a yield displacement of 4 mm and an ultimate displacement of 36 mm. Yield and ultimate displacements are subsequently used to derive the boundaries between damage grades (DG) as defined by the European Macroseismic Scale (EMS98) [14] and formulated for existing masonry buildings by Lagomarsino and Giovinazzi [15]. As data-driven damage assessment is most useful for buildings with low-to-moderate damage (heavy damage can be observed visually by non-expert inspectors) the study focuses on DGs 1 to 3. In addition, a DG0 is introduced in addition to the EMS98 DGs and corresponds to a fully linear and elastic behavior of the structure, unlike DG1 which contains slight nonlinearities (see Figure 1).

The nonlinear behavior model of the Tremuri formulation uses a damage parameter to model the post-yield stiffness of each macro-element of the equivalent frame. This parameter is used to monitor the nonlinearity of the structure (in order to validate the DSFs). The increasing nonlinearity (based on the damage coefficient inherent to the model) is represented in Figure 1 with the color shade of the pushover curve. Unlike the DSFs described in Section 2, stiffness reduction and damage parameters cannot be measured accurately in real structures and are only used for comparison with DSFs.

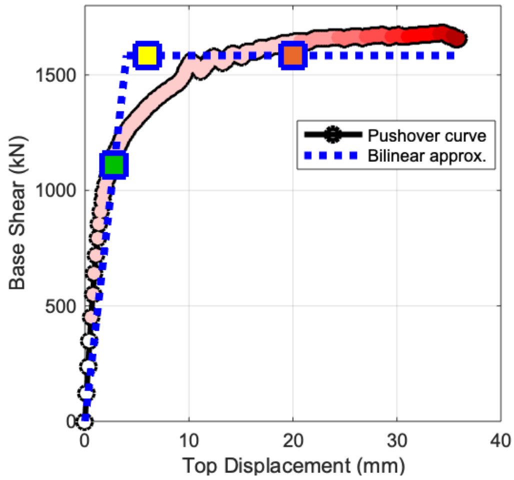

Figure 1. Simulated pushover curve of the masonry building and the corresponding bi-linear approximation (dotted line) with the delimitation of displacement-based damage-grades.

Subsequently the equivalent-frame model is used to simulate the dynamic response of the building to four historic ground motions with increasing amplitude: Montenegro 1979 (MNG), Northridge 1994 (NRG), Gilroy 2002 (GIL), L'Aquila 2009 (LAQ). In total, 50 ground motions are simulated. Acceleration responses at the top of the building are used as output signal, $\ddot{x}_o$, while the ground shaking is used as input signal, $\ddot{x}_i$. A constant Rayleigh-type damping is assumed for the dynamic simulations. In addition, neither strength degradation nor residual stiffness degradation are considered for the dynamic simulation of macro-elements of the equivalent frame model. Absence of residual stiffness degradation presents a complex case for data-driven nonlinearity detection as traditional approaches, such as residual changes in natural frequencies that could be found using ambient vibrations would fail to reveal such nonlinear behavior.

The evolution of the four DSFs, described in Section 2, with respect to spectral accelerations (computed as the mean between the spectral accelerations evaluated at the fundamental frequency and half of the fundamental frequency) is shown in Figure 2. All DSFs change with increasing S_a, indicating their potential to track behavior changes in the system.

The coherence-based DSF_{coh} (Figure 2a) shows good agreement for low spectral accelerations but diverges for higher spectral accelerations. However, it has to be noted that the changes in coherence are relatively small (< 10 %) which may reduce the accuracy in cases of higher noise (as may the case in real-world applications with low-cost sensors).

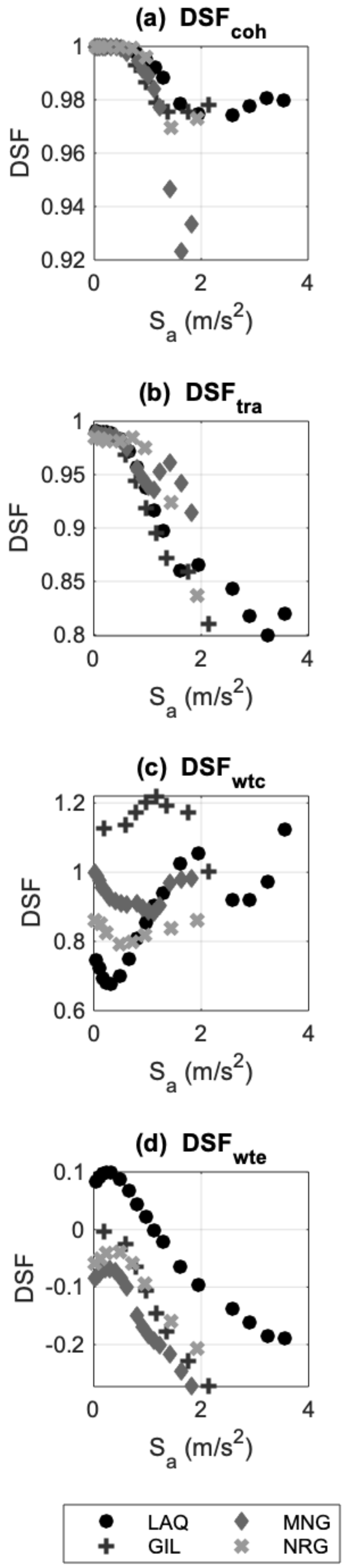

Figure 2. Evolution of the four damage sensitive features with increasing spectral accelerations (average value of spectral accelerations evaluated at the fundamental frequency, f1, and at half the fundamental frequency, f1/2).

The transmissibility-based DSF_{tra} (Figure 2b) shows good agreement for low values of spectral accelerations and decreases gradually with increasing S_a. Although the scatter in the derived DSFs resulting from the selected ground motion increases for higher spectral accelerations, a correlation between Sa and DSF can be observed.

The wavelet-based DSF_{wtc} (Figure 2c) is characterized by large scatter and correlates well with the spectral content of the earthquake, rather than the nonlinearity of the structural response.

The wavelet-based DSF_{wte} (Figure 2d) has an almost linear relationship between S_a and DSF. However, the value of the DSF is significantly influenced by the spectral content of the ground-shaking, as evidenced by the vertical scatter at similar spectral accelerations for the four earthquake signals.

Based on the observations made in Figure 2, it is found that DSF_{wtc} has little potential for damage detection in masonry buildings, which are characterized by high stiffness, relatively little ductility and considerable redundancy in the load-resisting system.

As a first step towards quantifying building damage, which is essential for applications such as automated smart tagging of buildings, DSFs are compared to the DGs that are derived for each simulated earthquake instance. This comparison is meaningful as the formulation of DGs is a generalized damage assessment over the entire building and the studied DSFs evaluate the global response based exclusively on acceleration signals from the base and the top of the building. The reference state of the studied building corresponds to fully linear elastic behavior and is labelled as DG0. DGs 1 to 3 are attributed using the maximum roof displacement, in accordance with the EMS98 damage-scale, as shown in Figure 1.

Figure 3 shows the values of DSF_{coh} that correspond to DGs 0 to 3. When the system remains linear, the value of DSF_{coh} remains at 1 and thus, successfully indicates absence of any damage or nonlinear behavior. When nonlinearity occurs, the value of the DSF drops below 1. Although the changes remain relatively small (< 10%), it is worth noting that due to software limitations the stiffness reduction occurs over a limited amount of time, without residual degradation.

The transmissibility-based DSF_{tra} (see Figure 4) shows similar behavior to DSF_{coh}, although the sensitivity to nonlinearity is higher (up to 20% reduction). When comparing DSF_{tra} and DSF_{coh} it appears that the earthquake signal does not influence the two indicators in the same way. While DSF_{tra} (Figure 3) produces singularities for the Northridge-earthquake signal (NRG) in DG1 and DG2, DSF_{coh} (Figure 4) is more sensitive to nonlinearities created by the signal corresponding to the L'Aquila earthquake (LAQ) in DG2. For a more robust classification of buildings into DGs after an earthquake, a combination of DSFs could therefore be considered.

The wavelet-based DSF_{wte} exhibits a large scatter for each DG, even for the linear DG0. As DSF_{wte} is based on the energy spread in the frequency domain of the structural response, it is much more influenced by the spectral content of the ground shaking. The DSF_{wte} in Figure 5 is presented as the relative change with respect to the undamaged reference case in order to provide meaningful values that can be interpreted by engineers. Positive values of DSF_{wte} result from a higher energy share at the natural frequency, f_1, which can result from slight resonance phenomena if the energy content of the ground motion in the vicinity of f_1 is higher.

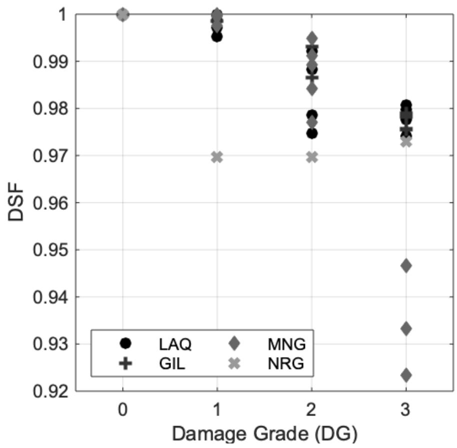

Figure 3. Values of DSF_{coh} corresponding to the simulated DGs.

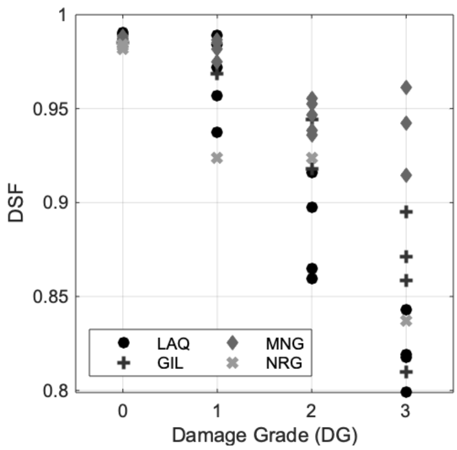

Figure 4. Values of DSF_{tra} corresponding to the simulated DGs.

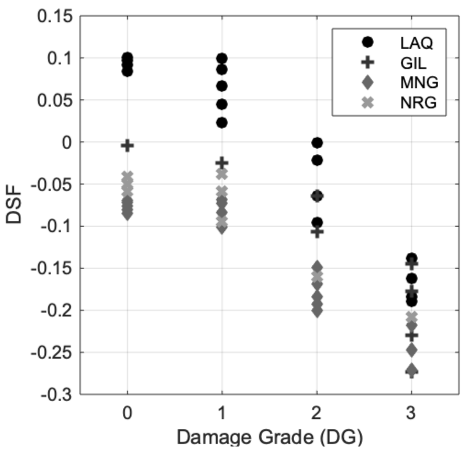

Figure 5. Values of DSF_{wte} corresponding to the simulated DGs.

The EMS98 DGs aim at a discrete classification of damage and therefore, each DG encompasses a range of displacement values and, by extension, levels of nonlinearity. In addition, higher DGs present larger intervals for the maximum roof displacement (see Figure 1), which inevitably results in larger scatter for DG2 and DG3 in continuous DSFs, as shown in Figures 3 to 5.Therefore, based on the damage factor that is used in the numerical model to account for nonlinearity, Figure 6 illustrates the relationship between the nonlinearity parameter (continuous variable) and the DSF_{tra}. For readability, elastic simulations (DG0) have been omitted from Figure 6. Compared with Figure 4, there is a clear trend in Figure 6 that higher nonlinearity leads to lower values of DSF_{tra} and the vertical scatter is therefore reduced. However, a correlation between the earthquake signal and the value of DSF_{tra} can be observed, as for instance the L'Aquila earthquake (LAQ) tends to lower values of DSF_{tra} for large values of nonlinearity (> 0.5) than the Gilroy earthquake (GIL). For changing amplitudes of a same earthquake signal, the evolution of the DSF with respect to nonlinearity is coherent.

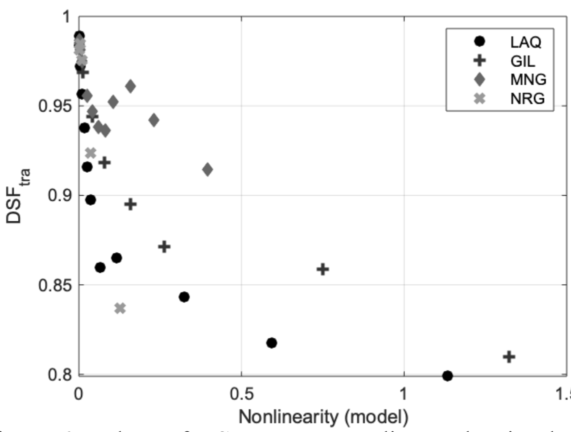

Figure 6. Values of DSF_{tra} corresponding to the simulated level of nonlinearity.

4 TESTING DAMAGE-SENSITIVE FEATURES ON SHAKE-TABLE DATA

Simulating the response of buildings contains many idealizations and simplifications when compared to real-world applications. Therefore, the DSFs are also tested with the data of a half-scale four-story building that has been tested on the EUCENTRE shake table in Pavia by Beyer et al. [16]. The response of the mixed, unreinforced-masonry and reinforced-concrete, building to the Montenegro 1979 earthquake, scaled to increasing levels of peak ground acceleration (PGA) has been measured.

White-noise excitation that has been applied to the structure prior to any earthquake shaking is used as reference state of the structure. The fundamental frequency in the (unilateral) direction of shaking is found to be 6.9 Hz and, based on the spectral analysis of the structural response to the white-noise excitation, the range of frequencies to compute the DSFs is taken as [4, 7.5] Hz.

The response of the building is analyzed separately for six levels of shaking (five increasing levels of shaking, with PGA ranging from 0.13g to 0.76g, followed by one after-shock with a PGA of 0.37g). The transmissibility function at the reference state and during the fourth earthquake (PGA=0.4) are given in Figure 7. The red symbols indicate the selected frequency range considered for the definition of the DSF_{tra}, . It can be seen that the transmissibility derived for the earthquake shaking has its peak and significant part of its energy spread shifted towards lower frequency values, which is a result of reduced.

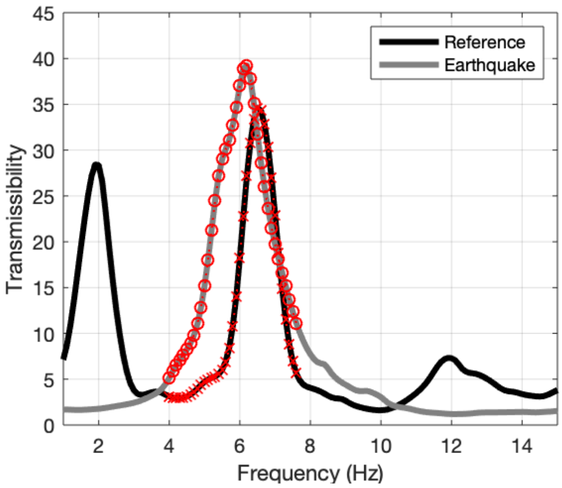

Figure 7. Transmissibility function derived for the reference case and the 4th earthquake instance. The selected frequency range for the definition of DSF_{tra} is highlighted with 'x' and 'o' symbols for the reference and earthquake signals respectively.

The values of DSF_{tra} as a function of PGA for the six levels of shaking are reported in Figure 8(a). Visual inspections performed on the specimen after each shaking test have concluded that the building remained in DG1 for the first 2 tests and in DG2 for the 4 subsequent tests, which include one aftershock. More information on the building state and the testing protocol can be found in [16].

As can be seen in Figure 8(a), DSF_{tra} accurately predicts little damage for the first two tests, with increasing levels of damage for the subsequent tests. Especially after the fifth test (PGA = 0.76g) DSF_{tra} indicates that the structure has sustained damage, which remains constant during the aftershock (DG2-AS in Figure 8). This is consistent with observations made from the specimen and highlights the potential of DSFs to track nonlinear behavior and provide a continuous quantification of the extent of damage. The behavior of DSF_{coh} is comparable to the behavior of DSF_{tra}, even though, as described in Section 3, the observed changes are lower (<20% compared to 80%).

The wavelet-based DSF_{wte} (shown in Figure 8b) also reveals a change in the structural state that initiates with the third earthquake, although the drop is much steeper compared with DSF_{tra}. Application to further experimental data is required in order to assess which DSF scales best with the real extent of damage. For robust assessment of damage in real buildings, a combination of several DSFs may prove the most suitable. As already noted for the simulated case study (Section 3), the DSF_{wtc} also reveals onset of damage with test number 3, which however does not show consistency with accumulating damage in subsequent tests.

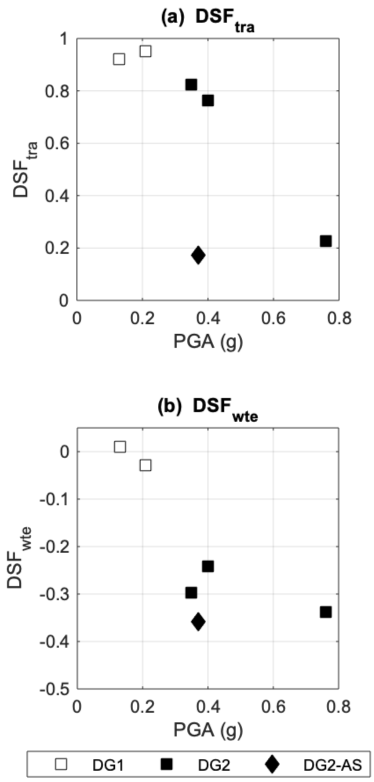

Figure 8. Evolution of DSF_{tra} (a) and DSF_{wte} (b) for increasing levels of shaking. The aftershock shaking (DG2-AS) has been applied to the specimen after the five previous shaking levels and thus, contains similar levels of damage than the previous shaking at PGA = 0.76g.

5 SUMMARY AND DISCUSSION

The potential of data-driven DSFs for detection and quantification of earthquake-induced damage is here illustrated through application on simulated earthquake responses of a three-dimensional model of an unreinforced masonry building, as well as on shake-table experiments performed on a half-scale four-story building. All DSFs exploit changes in the fundamental frequency of a building as a proxy of nonlinearity and thus, damage. However, different techniques are used to represent the building response in the frequency domain: transmissibility, magnitude-squared coherence and wavelet decomposition. Table 1 contains a summary of the four tested DSFs. Results have shown that the first three DSFs provide satisfactory results.

Table 1. Summary of the performance of the four tested DSFs.

DSF	Requires undamaged data	Required sensors	Robustness to input shaking
DSF_{tra}	Yes	2	Yes
DSF_{coh}	Yes	2	Yes
DSF_{wte}	Yes	1	No
DSF_{wtc}	Yes	2	No

DSFs have been shown to not only detect the onset of nonlinear behavior; they also scale with the extent of damage and therefore could provide a valuable contribution towards automated smart-tagging of buildings after an earthquake.

With well-chosen indicator buildings that are representative of properly defined building classes within a region, such smart-tagging could contribute to rapid loss assessment after earthquakes, thus increasing the resilience of the built environment by reducing down-time and speeding up recovery. With such building typologies, relationships between the extent of damage and DSFs can also be formulated in order to be able to include DSFs as engineering demand parameters (EDPs) into a probabilistic performance-based earthquake-engineering framework. While performance-based assessment with behavior models is required to not only assess the damage sustained by an earthquake, but also to conclude on the capacity of a building to withstand future earthquakes or strong aftershocks, application of the full chain of performance-based earthquake engineering (intensity measures, engineering demand parameters, performance groups, damage indicators) accumulates many uncertainties that can be alleviated with measurable DSFs. In addition, DSFs can be used as data-driven criteria for updating physics-based engineering models in order to reduce the uncertainty of model-based predictions of the residual seismic capacity of damaged buildings [17, 18].

While the application to the shake-table tests (Section 4) has shown that the studied DSFs can be applied to experimental datasets, such data do not include all sources of uncertainty that complicate real-world applications, such as environmental influences on material properties, amplitude-dependent elastic changes in stiffness and soil-structure interaction. These sources of uncertainty influence the spectral responses of buildings independently of damage and may result in false alarms. In addition, by comparing Sections 3 and 4, the limitation of the shake-table tests to different scaling of one ground-motion signal may provide an upper bound estimate of the performance of DSFs.

6 CONCLUSIONS

In this paper, four data-driven damage-sensitive features (DSF) are reviewed and applied to a simulated response of an unreinforced masonry building to earthquakes and to shake-table tests on a four-story buildings. The following conclusions are drawn with respect to DSFs that can be derived in near-real time from measurement data:

- DSFs that are based on changes in the frequency-domain of the dynamic response to earthquake loading detect the onset of damage in low-rise and stiff structures such as masonry buildings.
- DSFs that are obtained using 1 or 2 acceleration sensors scale with the extent of damage and therefore, have potential to be used for damage quantification and as input for data-driven model updating.
- Data-driven detection and quantification of damage requires reference recordings of the structure at healthy state (linear-elastic response).
- Spectral contents of the ground shaking influence the four frequency-based DSFs in different ways and therefore, one single DSF may not be sufficient to perform robust damage identification.

ACKNOWLEDGMENTS

The authors would like to thank Ravina Sriram, MSc student at ETH Zurich, for her contributions to the model of the case study. The research described in this paper was financially supported by the Real-time Earthquake Risk Reduction for a Resilient Europe 'RISE' project, financed under the European Union's Horizon 2020 research and innovation programme, under grant agreement No 821115, as well as the ETH Grant (ETH-11 18-1) DynaRisk - "Enabling Dynamic Earthquake Risk Assessment".

REFERENCES

[1] F. Vidal, M. Navarro, C. Aranda and T. Enomoto; *Changes in dynamic characteristics of Lorca RC buildings from pre-and post-earthquake ambient vibration data*, Bull. of Earthq. Eng., 12(5), 2095-2110, 2014.

[2] L. Cheng, J. Yang, D. Zheng, B. Li and J. Ren. *The health monitoring method of concrete dams based on ambient vibration testing and kernel principle analysis*. Shock and Vibration, 2015.

[3] H. S. Park and K. O. Byung. Damage detection of building structures under ambient excitation through the analysis of the relationship between the modal participation ratio and story stiffness. Journal of Sound and Vibration 418: 122-143, 2018.

[4] B. Moaveni, H. Xianfei, J. P. Conte and J. I. Restrepo. Damage identification study of a seven-story full-scale building slice tested on the UCSD-NEES shake table. Structural Safety 32, no. 5: 347-356, 2010.

[5] M. P. Limongelli, Seismic health monitoring of an instrumented multistory building using the interpolation method. Earthquake engineering & structural dynamics 43, no. 11: 1581-1602, 2014.

[6] Y-L Zhou, H. Cao, Q. Liu, and M. A. Wahab. Output-based structural damage detection by using correlation analysis together with transmissibility. Materials 10, no. 8: 866, 2017.

[7] M. Pastor, M. Binda, and T. Harčarik. "Modal assurance criterion." Procedia Engineering 48: 543-548, 2012.

[8] A.G. González, J. Rodrıguez, X. Sagartzazu., A. Schumacher, I. Isasa, . Multiple coherence method in time domain for the analysis of the transmission paths of noise and vibrations with non-stationary signals. Proceedings of Intern. Conference of Noise and Vibration Engineering, 3927-3941, 2010.

[9] H. Y. Noh, K. K. Nair, D. G. Lignos and A.S. Kiremidjian, *Use of wavelet-based damage-sensitive features for structural damage diagnosis using strong motion data*. Journal of Structural Engineering, 137(10), 1215-1228, 2011.

[10] H. Y. Noh, D. G. Lignos, K. K. Nair and A.S. Kiremidjian. Development of fragility functions as a damage classification/prediction method for steel moment-resisting frames using a wavelet-based damage sensitive feature. Earthq. Eng. & Structural Dynamics, 41(4), 681-696, 2012.

[11] Y. Reuland, A.A. Jaoude, P. Lestuzzi, and I.F.C. Smith *Usefulness of ambient-vibration measurements for seismic assessment of existing structures*. In Proceedings of the 4th Intern. Conf. on Smart Monitoring, Assessment and Rehabilitation of Civil Structures, Zurich, 2017.

[12] A. Lagomarsino, A. Penna, A. Galasco, S. Cattari, TREMURI program: An equivalent frame model for the nonlinear seismic analysis of masonry buildings Engineering Structures, Vol. 56, 1787-1799, 2013.

[13] A. Penna, S. Lagomarsino, A. Galasco, *A nonlinear macroelement model for the seismic analysis of masonry buildings*, Earthquake Engineering and Structural Dynamics, Vol. 43(2), 159-179, 2014.

[14] G. Grünthal, R.M.V. Musson, J. Schwarz, M. Stucchi, *European Macroseismic Scale 1998, EMS-98*. Cahiers du Centre Européen de Géodynamique et de Séismologie, Volume 19; 2001.

[15] S. Lagomarsino and S. Giovinazzi, Macroseismic and mechanical models for the vulnerability and damage assessment of current buildings. Bulletin of Earthquake Engineering, 4(4), 415-443, 2006.

[16] K. Beyer, M. Tondelli, S. Petry and S. Peloso; Dynamic testing of a four-storey building with reinforced concrete and unreinforced masonry walls: prediction, test results and data set. Bulletin of Earthquake Engineering, 13(10), 3015–3064, 2015.

[17] Y. Reuland, P. Lestuzzi, and I.F.C. *Smith. Measurement-based support for post-earthquake assessment of buildings*. Structure and Infrastructure Engineering 15(5), 647-662, 2019.

[18] I. Iervolino, E. Chioccarelli, and A. Suzuki. *Seismic damage accumulation in multiple mainshock–aftershock sequences.* Earthquake Engineering & Structural Dynamics, 2020.